Journal of Bioenergetics and Biomembranes, Vol. 24, No. 1, 1992

Minireview

FTIR Difference Spectroscopy of Bacteriorhodopsin: Toward a Molecular Model

Kenneth J. Rothschild[1]

Received October 28, 1991

Bacteriorhodopsin (bR) is a light-driven proton pump whose function includes two key membrane-based processes, active transport and energy transduction. Despite extensive research on bR and other membrane proteins, these processes are not fully understood on the molecular level. In the past ten years, the introduction of Fourier transform infrared (FTIR) difference spectroscopy along with related techniques including time-resolved FTIR difference spectroscopy, polarized FTIR, and attenuated total reflection FTIR has provided a new approach for studying these processes. A key step has been the utilization of site-directed mutagenesis to assign bands in the FTIR difference spectrum to the vibrations of individual amino acid residues. On this basis, detailed information has been obtained about structural changes involving the retinylidene chromophore and protein during the bR photocycle. This includes a determination of the protonation state of the four membrane-embedded Asp residues, identification of specific structurally active amino acid residues, and the detection of protein secondary structural changes. This information is being used to develop an increasingly detailed picture of the bR proton pump mechanism.

KEY WORDS: Proton transport; biomembranes; infrared; membrane protein; energy transduction.

INTRODUCTION

An important goal in membrane biology and biophysics is to determine how membrane proteins function as energy transducers and active ion transporters. Since the early 1970's, when W. Stoeckenius and coworkers first established that bacteriorhodopsin (bR) functions as a light-driven proton pump, bR has become a major focus of this research. Several factors that have contributed to this interest in bR include its relatively small size (26,000 MW), ease of production, thermal and photochemical stability, a retinylidene chromophore with a visible absorption, and a photocycle consisting of several metastable intermediates. In addition, bR forms a two-dimensional crystalline lattice which enables the use of scattering techniques to probe the structure of bR (Henderson and Unwin, 1975).

Interest in understanding the proton pumping mechanism of bR has also been stimulated by the discovery of other retinal-containing membrane proteins from *Halobacterium halobium*, including halorhodopsin, a light-driven chloride pump, and sensory rhodopsin I, a phototactic receptor. Since these proteins and bR have similarities in their primary sequences (Blanck and Oesterhelt, 1987; Blanck *et al.*, 1989), it is likely that they share common features in their respective mechanisms despite differences in their function. Bacteriorhodopsin also has potential uses in biotechnology, including in advanced nonlinear optoelectronic materials, holographic recording media, neural networks, and chemical detectors (Birge *et al.*, 1989; Rayfield, 1989; Haronian and Lewis, 1991; Uehara *et al.*, 1990; Birge, 1990; Hampp *et al.*, 1990).

In this review, we describe the application of Fourier transform infrared (FTIR) difference spectro-

[1]Departments of Physics and Physiology and the Program in Cellular Biophysics, Boston University, 590 Commonwealth Avenue, Boston, Massachusetts 02215.

0145-479X/92/0400-0147$06.50/0

scopy in conjunction with other techniques, with special emphasis on site-directed mutagenesis (Khorana, 1988), to investigate the proton-pumping mechanism of bacteriorhodopsin (bR). In the past decade, this approach has helped provide an increasingly detailed picture of the proton-pump mechanism. These studies have also demonstrated the usefulness of FTIR difference spectroscopy for investigating other membrane proteins. A detailed discussion of some of the technical aspects of FTIR and related methods including ATR, polarized FTIR, and time-resolved FTIR will not be given here (see Braiman and Rothschild, 1988; Rothschild, 1988; Kitagawa and Maeda, 1989). We will also not discuss complementary spectroscopic techniques such as time-resolved visible absorption, resonance Raman spectroscopy, and solid-state NMR, which have also contributed to our current knowledge of the bR proton-pump mechanism.

FTIR AS A PROBE OF INDIVIDUAL AMINO ACID RESIDUES

Several features of infrared spectroscopy make it an attractive technique for studying bacteriorhodopsin. In contrast to resonance Raman spectroscopy, which uses visible light to selectively probe the structure of the retinylidene chromophore (Smith *et al.*, 1985), infrared radiation is absorbed by all components of the protein, including amino acid residues and the chromophore. For this reason, information can be obtained which complements resonance Raman spectroscopy. Because the absorbed infrared light can be polarized, it can be used to probe the orientation of specific chemical groups. Infrared also has an intrinsic time resolution in the picosecond range, providing a window on fast molecular processes.

Since the development of the modern Fourier transform infrared spectrometer (Griffiths and de Haseth, 1986), dramatic improvements have been made in the sensitivity of infrared spectroscopy. Whereas a normal grating spectrometer is essentially a filter which allows light of only a selected frequency to pass through (rejecting all other photons), a Fourier transforming spectrometer processes light of all frequencies simultaneously, storing the information as an interferogram. Since fewer photons are lost in a Fourier transform system, a higher resolution spectrum can be built up faster than in a grating system.

The first application of FTIR to purple membrane was reported in 1979, where the secondary structure in bR was investigated by measuring the infrared dichroism of oriented samples (Rothschild and Clark, 1979). This study and a related work (Rothschild *et al.*, 1980) confirmed earlier electron diffraction measurements (Henderson and Unwin, 1975) which revealed a bulk structure of bR consisting of α-helix-like tubes which had a net orientation perpendicular to the membrane plane. The discovery of an anomalous amide I frequency near 1661 cm^{-1} (Rothschild and Clark, 1979; Rothschild *et al.*, 1980) also raised the possibility of an unusual or distorted α-helix conformation (Rothschild *et al.*, 1980; Krimm and Dwivedi, 1982) as discussed recently in several recent reports (Glaeser *et al.*, 1991; Earnest *et al.*, 1990; Gibson and Cassim, 1989; Hunt *et al.*, 1988).

A number of groups have used FTIR in combination with resolution enhancement methods to study the secondary structure of bR. In one comparative study of bacteriorhodopsin, rhodopsin and Ca^{+2}-ATPase, second-derivative spectroscopy (Lee *et al.*, 1985) revealed in all three proteins the appearance of bands near 1640 and 1525 cm^{-1}, characteristic of β-structure. However, the existence of significant levels of β-structure in bR has been a matter of controversy with conflicting reports based on IR, UV, circular dichroism, and electron diffraction data (Jap *et al.*, 1983; Downer *et al.*, 1986; Nabedryk and Breton, 1986; Glaeser *et al.*, 1991).

Recently, the secondary structure of bacteriorhodopsin has been examined by combining polarized FTIR with the methods of hydrogen/deuterium exchange, isotope labelling, and resolution enhancement (Earnest *et al.*, 1990). It was found that the dichroism of amide I and II bands, which reflects the net orientation of the bR α-helices, was unchanged even though the protein exhibited extensive H/D exchange of amide groups. These results demonstrate that there exists a well-oriented α-helical "core" structure in bR which is resistant to H/D exchange, whereas surface regions contain β-type structure. It was also found that components of the amide I and II bands, whose frequency is characteristic of β-structure (Haris and Chapman, 1988), have strong contributions from the C=C ethylenic stretch and C=N Schiff base modes of the chromophore (Earnest *et al.*, 1987, 1990). An extension of this approach is currently being applied to investigate the mechanism of membrane protein folding and the forces which stabilize membrane protein structure. In this work, proteolytic and synthetic

fragments of bR are reconstituted into model membranes and the structure, orientation, and H/D exchange rates are determined by polarized FTIR spectroscopy (Hunt *et al.*, 1991).

FTIR Difference Spectroscopy

While infrared spectroscopy offers a window on the conformation and dynamics of biological molecules, in practice it can be difficult to detect localized structural changes of individual groups. This problem stems from the existence of strong overlap between the frequency of the vibrational modes of the many similar groups in a protein. For example, the infrared spectrum of a protein in the 1500–1700 cm^{-1} region has contributions from all of the amide groups which produce the strongly infrared-active amide I and II modes (Parker, 1983) as well as vibrational modes from side-chain vibrations of several amino acid residues including aspartate, glutamate, tyrosine, tryptophan, lysine, and arginine (Venyaminov and Kalnin, 1990). This overlap makes it extremely difficult to resolve the contribution of a single amino acid residue in a protein infrared spectrum.

One simple approach to this problem is based on the principle of *difference spectroscopy* (cf. Fig. 1). FTIR spectra are recorded for two different states of the protein, and the difference spectrum of these two states is computed. In the case of bacteriorhodopsin, these states can consist of the light-adapted form (bR_{570}) and one of the photocycle intermediates. This approach was first reported in 1981, where the bR → M difference spectrum was measured (Rothschild *et al.*, 1981). By comparing this difference spectrum with that obtained from resonance Raman spectroscopy of bR as well as through the use of isotope labelling and H/D exchange, specific bands in the spectrum could be assigned to protein and chromophore vibrational modes. This work and several other early studies of the bR → K, L and M transitions (Rothschild and Marrero, 1982; Bagley *et al.*, 1982; Siebert and Mäntele, 1983) demonstrated the ability of this method to detect small structural changes in both the chromophore and the protein components of bR.

All of the early FTIR difference measurements on bR used low temperature or partial dehydration in order to trap specific intermediates in the photocycle (Rothschild *et al.*, 1981; Rothschild and Marrero, 1982; Bagley *et al.*, 1982; Siebert and Mäntele, 1983). While this method, sometimes termed static FTIR difference spectroscopy, has contributed to our current knowledge about the structural changes in bR, the conditions used can cause blocks in structural transitions of the protein (Braiman *et al.*, 1987). More recently, the development of time-resolved FTIR techniques (Braiman *et al.*, 1987; Gerwert *et al.*, 1990b; Braiman *et al.*, 1991; Bousché *et al.*, 1991a) has allowed FTIR difference spectra of bR to be obtained at room temperature, complementing time-resolved single-wavelength kinetic methods (Mäntele *et al.*, 1982). The results of some of these studies will be discussed in the next section.

In addition to bR, the closely related membrane proteins, halorhodopsin (Rothschild *et al.*, 1988) and sensory rhodopsin I (Bousché *et al.*, 1991b) from *Halobacterium halobium*, as well as the visual rhodopsins (Rothschild *et al.*, 1983; Siebert *et al.*, 1983; Bagley *et al.*, 1985; Rothschild and DeGrip, 1987; DeGrip *et al.*, 1988), have been analyzed using this method. Non-retinal containing light-triggered proteins extensively analyzed include cytochrome oxidase (Alben *et al.*, 1982) and the photosynthetic reaction center (Nabedryk *et al.*, 1990). Recently, FTIR difference spectroscopy has been extended to investigate proteins which are not activated by light, including Ca^{2+}-ATPase (Barth and Mäntele, 1991) and the nicotinic acetylcholine receptor (nAChR) (Baenziger *et al.*, 1992).

The growing application of FTIR difference spectroscopy to membrane proteins several related techniques including:

1. Polarized FTIR difference spectroscopy to probe the orientational changes of specific groups in a protein (Earnest *et al.*, 1986; Nabedryk and Breton, 1986; Breton and Nabedryk, 1989; Fahmy *et al.*, 1989).
2. Time-resolved FTIR difference spectroscopy (Braiman *et al.*, 1987; Gerwert and Hess, 1988; Braiman and Wilson, 1989; Gerwert *et al.*, 1990b; Braiman *et al.*, 1991; Uhmann *et al.*, 1991).
3. Attenuated total reflection FTIR difference spectroscopy to probe conformational and protonation changes of membrane proteins in an aqueous environment (Marrero and Rothschild, 1987a, b; Yang *et al.*, 1987).
4. Resolution enhancement and isotope labelling to identify bands due to single residues in the absolute infrared absorption spectrum (Lee *et al.*, 1985; Earnest *et al.*, 1987, 1990).

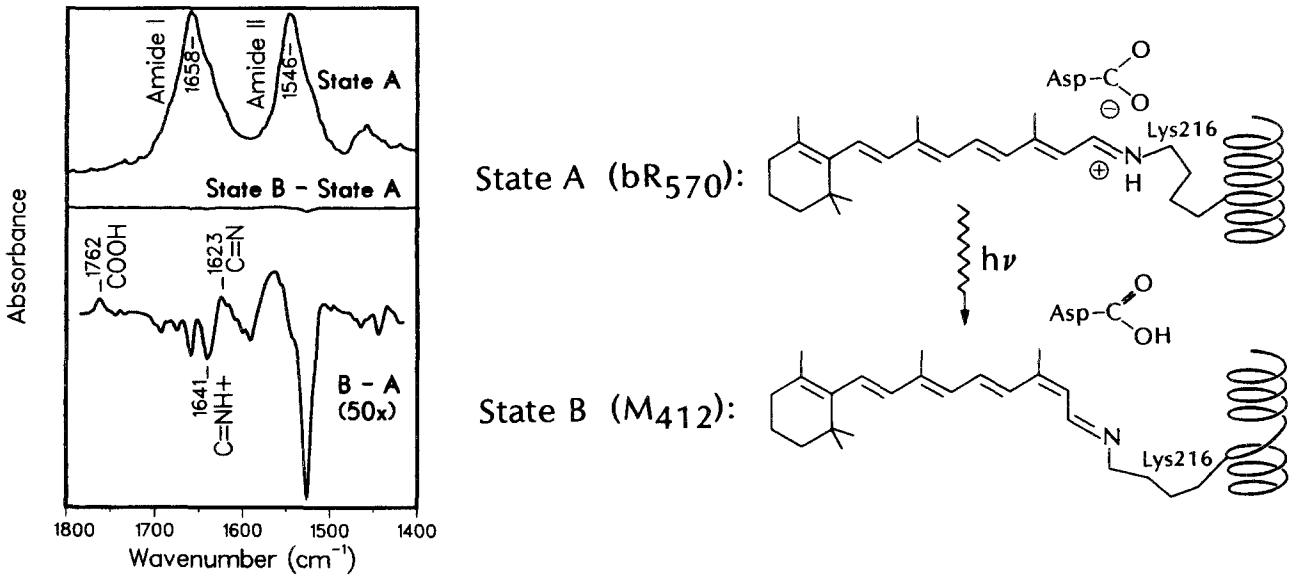

Fig. 1. FTIR difference spectroscopy as applied to bR. Right, simplified structure of the active site of bR (State A, bR_{570}) showing the retinylidene chromophore attached to helix F through a protonated Schiff base formed with Lys-216. (State B, M_{412}) involves isomerization of *all-trans*-retinal to 13-*cis*, and transfer of a proton from the retinal-Lys-216 Schiff base bond to the Asp-85 counterion. Left, the IR spectrum of bR_{570} obtained in the dark at $-20°$ (top), and the light-minus-dark difference spectrum on the same scale (middle) and a $50\times$ expanded scale (bottom) (from Braiman and Rothschild, 1988).

While these methods will not be covered explicitly in this review, several examples are given in the research described below.

Methods of Assigning Bands in the FTIR Difference Spectrum

The ability of FTIR to provide detailed information about membrane protein mechanisms depends critically on the development of methods for assigning bands in the FTIR difference spectrum to individual groups.

Chromophore Vibrations

Chromophore bands in the FTIR difference spectrum of bR can be assigned by isotopically labelling retinal, similar to methods employed extensively in conjunction with resonance Raman studies (Smith *et al.*, 1985). A comparison of the resonance Raman and FTIR difference spectra can also facilitate assignments of chromophore vibrations in the FTIR difference spectrum. For example, such a comparison was made for the bR → K transition at low temperature of bR and bR containing 15-deuterio-retinal (Rothschild *et al.*, 1984a). This work led to the assignment of the most intense bands in the FTIR difference spectrum to the chromophore vibrations, indicating that at 77 K the major structural changes in bR during the bR → K transition involve the chromophore. Agreement in the *intensity* of the skeletal polyene bands found in the resonance Raman and FTIR difference spectra also revealed significant bond polarity throughout the retinal polyene chain (Rothschild *et al.*, 1984a).

Amino Acid Side-Chain Vibrations

Probing bacteriorhodopsin at the level of single amino acid residues requires that bands in the infrared spectrum be assigned to individual groups in the protein. This can be accomplished by the application of isotope labelling and site-directed mutagenesis in combination with FTIR difference spectroscopy (Braiman *et al.*, 1988a, b; Gerwert *et al.*, 1989).

The general approach, which is outlined in Fig. 2, involves first assigning bands in the infrared difference spectrum to a particular amino acid using isotope

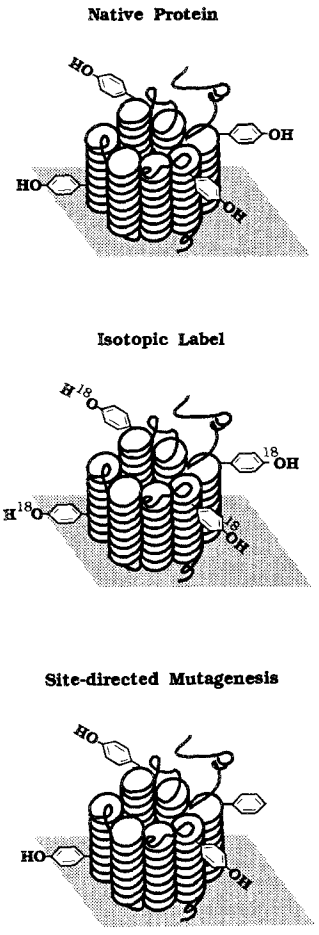

Fig. 2. Methods used to assign bands to specific tyrosine residues in the FTIR difference spectrum of a protein. (Adapted from He *et al.*, 1991.)

label incorporation. For example, incorporation of ^{15}N-proline provided the first direct evidence that prolines are structurally active in bR (Rothschild *et al.*, 1989c; Gerwert *et al.*, 1990a). A similar approach has resulted in assignments of bands to Asp, Tyr, Trp, and Lys amino acid residues (Engelhard *et al.*, 1985; Rothschild *et al.*, 1986; Dollinger *et al.*, 1986a; Eisenstein *et al.*, 1987; Roepe *et al.*, 1987a, b, 1988a; McMaster and Lewis, 1988).

Once bands due to an amino acid residue are assigned, the particular residue which gives rise to these vibrations can be identified by examining a set of mutants which involves this particular amino acid (Fig. 2). For example, in the first such study of this type (Braiman *et al.*, 1988b), all of the 11 Tyr residues were individually replaced by Phe and the bR → K and bR → M phototransitions measured by FTIR difference spectroscopy. This led to the assignment of the negative 1277 cm^{-1} band to Tyr-185 (Braiman *et al.*, 1988a) (see below). Several additional examples are given in the next section.

Thus far, several bands in FTIR difference spectra have been assigned to individual tyrosine, aspartic acid, and tryptophan residues using this approach (Fig. 3). These assignments provide information about the changes which individual residues undergo at specific steps in the bR photocycle and have facilitated development of an increasingly detailed model of the bR proton pump (Braiman *et al.*, 1988a; Rothschild *et al.*, 1989b, 1990a, 1992).

SELECTED RESULTS

In this section, we describe several selected results which will be discussed in the next section in the context of a bR proton transport model. The reader is also directed to references herein on FTIR studies from other laboratories along with three earlier reviews (Braiman and Rothschild, 1988; Rothschild, 1988; Kitagawa and Maeda, 1989).

Evidence for an Alteration in the Environment of the Schiff Base in the bR → K Transition

The frequency of the Schiff base C=N bond can be used to probe the environment and structure of the Schiff base during the bR photocycle. In the case of the K intermediate, this mode was assigned using isotope labelling to a component of the positive band at 1609 cm^{-1} (Rothschild *et al.*, 1984b) or 1613 cm^{-1} (Gerwert *et al.*, 1985) a shift of approximately 30 cm^{-1} below that of bR_{570}. Much of this shift can be attributed to increased delocalization of electrons throughout the polyene chain which also correlates with an increased red-shifted λ_{max} (Aton *et al.*, 1980). However, the NH in-plane bending mode, whose frequency depends on the strength of hydrogen bonding to the Schiff base, can also have a large effect on the C=N vibrational frequency through coupling of the two vibrations (Aton *et al.*, 1980; Rodman *et al.*, 1990). In general, the results indicate a weakening of the interaction of the Schiff base with a counterions during the bR → K transition.

A change in the structure of the K chromophore at 77 K (low-K) and 135 K (high-K) has also been detected by FTIR, with the C=C and C=N stretching modes and the hydrogen-out-of-plane (HOOP) mode shifting up in frequency at the higher temperature (Rothschild *et al.*, 1985). It is likely that these changes

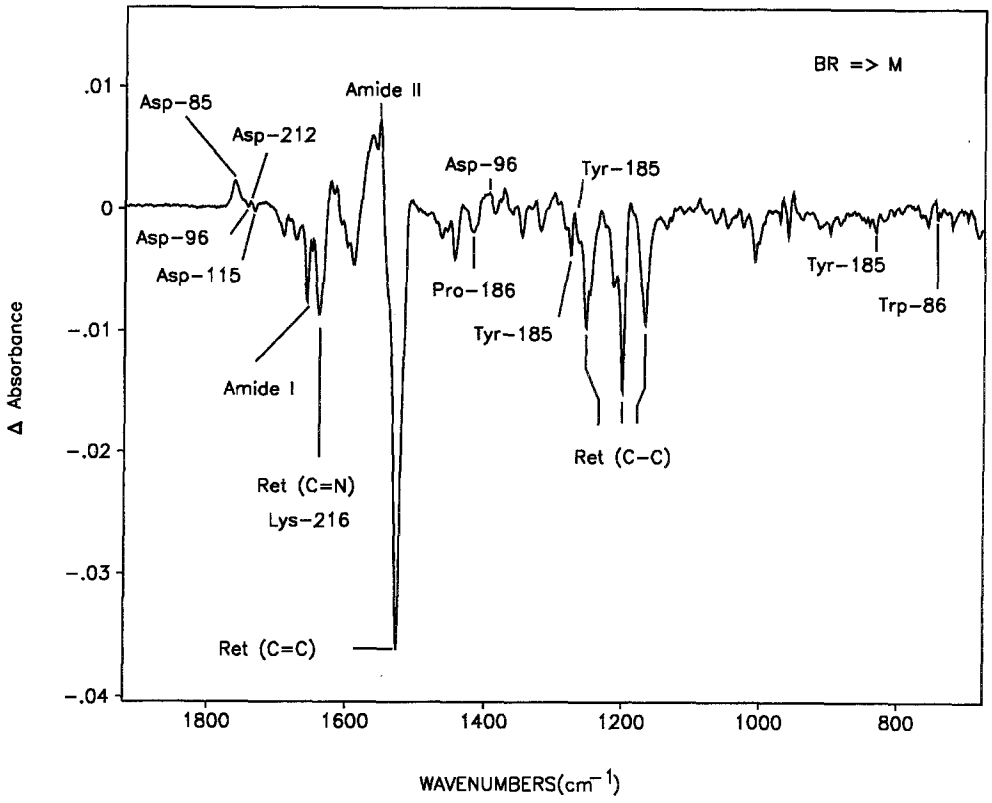

Fig. 3. Br → M FTIR difference spectrum recorded at 250 K showing assignments of vibrations from the retinylidene chromophore (RET) along with specific amino acid residues.

(Rothschild *et al.*, 1985). It is likely that these changes reflect the ability of the chromophore to adopt a more relaxed configuration at higher temperature possibly due to a conformational change of the protein. Interestingly, recent evidence indicates the same change occurs *temporally* in the early stages of the bR photocycle. In particular, the 77 K low-temperature FTIR difference spectrum is very similar to the room-temperature picosecond kinetic IR spectrum recently obtained in the 1550–1700 cm^{-1} region (Diller *et al.*, 1991). In contrast, the low-temperature FTIR difference spectrum at 135 K closely matches the chromophore bands assigned in the resonance Raman spectrum of the K chromophore at room temperature in

Assignment of a Band to Tyr-185: The First Combined Use of FTIR-Difference Spectroscopy and Site-Directed Mutagenesis

Several early studies based on UV absorption and fluorescence spectroscopy led to the suggestion that tyrosine protonation changes occur during the bR photocycle (Kalisky *et al.*, 1981; Bogomolni, 1980; Hanamoto and El-Sayed, 1984). This possibility was supported by FTIR studies which resulted in the assignment of tyrosine and tyrosinate bands in the bR → K, L, M and light–dark difference spectra (Rothschild *et al.*, 1986; Dollinger *et al.*, 1986a; Roepe *et al.*, 1987a, 1988b). For example, the introduction of the labels [L-ring-4-^{13}C-Tyr], [L-ring-$^{2}H_4$-Tyr], and [L-ring-$^{2}H_2$-Tyr] causes a shift in frequency of a band at 1277 cm^{-1} (negative) characteristic of the CO^- stretch mode of tyrosinate (Rothschild *et al.*, 1986; Dollinger *et al.*, 1986a). The frequency of this band is also insensitive to H/D exchange as expected for a tyrosinate. In contrast, several positive bands assigned to tyrosine shift upon H/D exchange. These results, along with UV absorption data (Rothschild *et al.*, 1986; Roepe *et al.*, 1987a), led to the conclusion that a tyrosinate group exists in light-adapted bR and that it protonates upon K formation. Additional changes in tyrosine protonation were also deduced from low-temperature (Rothschild *et al.*, 1986; Dollinger *et al.*, 1986a) and room-temperature bR → M difference spectra (Braiman *et al.*, 1987).

In order to assign the 1277 cm^{-1} band to a particular tyrosine residue in the bR primary sequence, Tyr → Phe substitutions were made at each of the 11 tyrosines in bR (Braiman *et al.*, 1988b). Since the 1277 cm^{-1} band disappeared in only the Tyr-185 → Phe substitution, the band was assigned to Tyr-185 (Braiman *et al.*, 1988b). Strikingly, this residue is located in the two-dimensional folding sequence of bR directly adjacent to Lys-216, the Schiff base linkage to the chromophore, thus supporting the model that Tyr-185 interacts with the Schiff base (Rothschild *et al.*, 1986). As discussed later, this information was used in the development of a spectroscopically derived model for the structure of the retinal binding site (Rothschild *et al.*, 1989a).

Since tyrosine has a pK_a close to 10.5, an important question concerns the absolute level of tyrosinate in light-adapted bR. In this regards, solid-state NMR has not detected the existence of tyrosinates in light-adapted bR (Herzfeld *et al.*, 1990), while conflicting results have been obtained from two different UV-enhanced resonance Raman studies (Ames *et al.*, 1990; Harada *et al.*, 1990). These studies raise the possibility that bands detected in the FTIR difference spectrum arise from a highly perturbed tyrosine(s) which has vibrational modes similar to a tyrosinate. Alternatively, it is possible that if only a small fraction of Tyr-185 is ionized in light-adapted bR, it would not be easily detectable by these techniques in contrast to FTIR difference spectroscopy which measures the net change in the ionization state of tyrosine during the bR → K transition.

In support of the latter possibility, it has recently been possible to estimate the level of tyrosinate in light-adapted bR by measuring the intensity of the 1277 cm^{-1} band in the absolute absorption spectrum (He *et al.*, 1992a). The assignment of this band to Tyr-185 was confirmed by measuring the absolute FTIR absorption spectrum of both bR containing an ^{18}O-Tyr label and the bR mutant Y185F expressed in native *Halobacterium halobium* (He *et al.*, 1992a). This led to an estimate of 0.4 tyrosinates/bR at 77 K with a further significant decrease from this level occurring at higher temperature (Y. W. He *et al.*, 1992b). As discussed below, this result is consistent with a model in which Tyr-185 participates in a hydrogen bond network with large proton polarizability resulting in a partial ionization of this residue and rapid equilibrium with its protonated form (Rothschild *et al.*, 1990a, 1992; He *et al.*, 1991). While FTIR, which has an intrinsic picosecond time resolution, would detect two distinct species in this case, the NMR spectrum would reflect a structure which is an average of the two equilibrating species.

Light-Driven Proton Transport Involves Protonation Changes of Aspartic Acid Residues 85, 96, and 212

The carboxyl groups of Asp and Glu could serve as key components in a proton-transporting hydrogen-bonding network (Eigen and DeMayer, 1958; Nagle and Tristram-Nagle, 1983; Zundel, 1988). The finding of a positive band at 1760 cm^{-1} in the FTIR difference spectrum of the bR → M transition (Rothschild *et al.*, 1981) provided the first evidence of protonation changes in the bR photocycle involving such groups. Subsequent studies using isotopic labels of Asp and Glu (Engelhard *et al.*, 1985; Dollinger *et al.*, 1986b) led to the assignment of this band and others which appear in the 1700–1760 cm^{-1} region of the bR → K, L, and M difference spectra to protonation or environmental changes of Asp residues. Static FTIR and kinetic infrared spectroscopy also helped establish the sequence of protonation changes which occur during the early photocycle (Mäntele *et al.*, 1982; Dollinger *et al.*, 1986b; Engelhard *et al.*, 1985; Roepe *et al.*, 1987a).

Site-directed mutagenesis and FTIR difference spectroscopy led to the first assignment of the carboxyl stretch bands in the bR → K, bR → L, and bR → M difference spectra to individual Asp residues (Braiman *et al.*, 1988a). Mutants of the four membrane-embedded Asp residues, Asp-85, Asp-96, Asp-115, and Asp-212, were examined. Table I shows the assignments and the protonation changes deduced from these measurements. On the basis of this information and related structure–function studies (Mogi *et al.*, 1988; Stern *et al.*, 1989), a proton-pumping model for bR was proposed (Fig. 4) (Braiman *et al.*, 1988a). A key feature of this model was the existence of an "active site" which included ionized Asp-212 and Asp-85 interacting with positively charged Arg-82 and the protonated Schiff base. The arrangement of these residues and the position of a neutral Asp-96 located 10 Å above the Schiff base provided the basis for a proton pump mechanism that is described in more detail in the next section.

While these studies were made using bR mutants produced in *E. coli* and reconstituted into native lipids, almost identical results were obtained from the mutants D96G and D96N expressed in native *Halobacterium halobium* (Gerwert *et al.*, 1989). Both

Table I. Protonation States of the Four Membrane-Embedded Asp Residues during the bR Photocycle (Adapted from Braiman *et al.*, 1988b)[a]

	bR	K	L	M	N	O
Asp-85	COO^-	COO^-	COO^-	COOH	COOH′	COOH′
Asp-96	COOH	COOH	$COO^- \rightleftharpoons$ COOH′	COOH′	COO^-	COOH
Asp-115	COOH	COOH′	COOH′	COOH′	COOH′	COOH
Asp-212	COO^-	COO^-	COO^-	$COO^- \rightleftharpoons$ COOH	$COO^- \rightleftharpoons$ COOH	$COO^- \rightleftharpoons$ COOH

[a]The COOH′ indicates a change of environment.

studies concluded that Asp-96 was protonated in light-adapted bR and underwent a change in environment upon M formation. However, as seen in Table I and Fig. 4, the evidence also suggested that Asp-96 undergoes a transient deprotonation during the lifetime of the L intermediate in agreement with recent submillisecond FTIR infrared measurements (Braiman *et al.*, 1991).

Trp-86 is Altered during the Primary Phototransition

In order to investigate the role of tryptophan residues in the bR photocycle, L-Trp containing a perdeuterated indole ring [L-$^2H_5$-Trp] was incorporated into bR, and the bR → K, L, and M transitions were measured by FTIR difference spectroscopy at low temperature (Roepe *et al.*, 1988a). Two negative bands at 742 and 756 cm^{-1} in the bR → K, L, and M difference spectra were found to arise from a strongly infrared active hydrogen out-of-plane (HOOP) mode of the indole ring of one or more tryptophans which are perturbed during the bR photocycle.

FTIR difference spectra were subsequently obtained for the bR → K and M photoreactions of bR mutants of all eight tryptophans in the bR sequence. None of the tryptophan residues were found to be essential for forming a normal light-adapted species with a 570 nm absorption. The 742 cm^{-1} band previously assigned to Trp was identified as arising from Trp-86. On this basis, it was concluded that Trp-86 was structurally active and perturbed during the primary photoreaction. In addition, a refined model of bR retinal binding pocket was proposed in which Trp-86, Trp-182, and Trp-189 form a "box" around the retinal chromophore to prevent chromophore photoisomerization other than at the C_{13}=C_{14} double bond (Rothschild *et al.*, 1989b) (Fig. 5).

Proline Residues Are Structurally Active in bR

It has been suggested that transport by membrane proteins involves proline residues which undergo structural alterations including isomerization about the Xaa-Pro peptide bond (Brandl and Deber, 1986) (where Xaa is an unspecified amino acid) or protonation at the imino nitrogen (Dunker, 1982). Structural changes involving bR proline residues were investigated by incorporating either a ring-perdeuterated proline or ^{15}N-labelled proline into bR and comparing the difference spectra obtained from the photoreactions of these labelled bR samples with those of unlabelled bR (Rothschild *et al.*, 1989c). This work and a second study (Gerwert *et al.*, 1990a) led to the assignment of bands due to proline vibrations in the 1420–1440 cm^{-1} region of the bR → K and bR → M difference spectra. The results indicate that one or more prolines undergo a structural rearrangement involving the Xaa-Pro C—N peptide bond during the bR photocycle. Since prolines changes are initiated during the bR → K photoreaction, an interesting possibility is that they are involved in coupling the light-induced isomerization of the retinal chromophore to protein secondary structural changes.

In a subsequent study (Rothschild *et al.*, 1990b), Fourier transform infrared difference spectroscopy in combination with site-directed mutagenesis was used to study the three membrane-embedded proline residues, Pro-50, Pro-91, and Pro-186. As in an earlier structure–function study of these residues (Mogi *et al.*, 1989), all three prolines were replaced by alanine and glycine; in addition, Pro-186 was changed to valine. Difference spectra were recorded for the bR → K and bR → M photoreactions of each of these mutants and compared to wild-type bacteriorhodopsin. Only substitution of Pro-186 caused significant perturbations in the frequency of the C=C and C—C stretching modes of the retinylidene chromophore. In addition, the Pro-186 substitutions reduced or abolished bands in the amide I and II region associated with secondary structural changes and altered signals assigned to the adjacent Tyr-185.

These results are consistent with a model of the retinal binding site in which Pro-186 and Tyr-185 are located in direct proximity to the chromophore

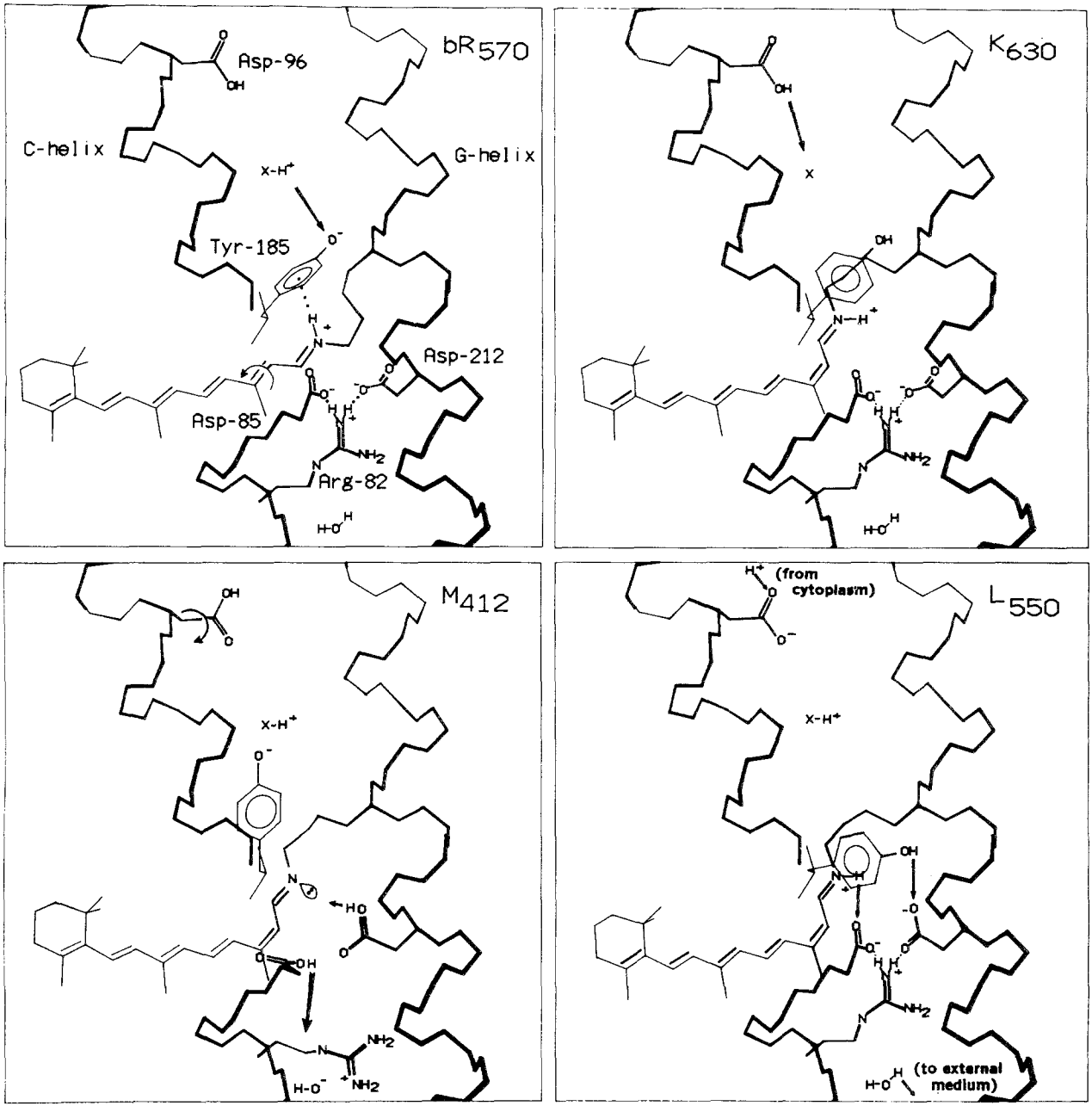

Fig. 4. The proton pumping mechanism and structural model for bR proposed on the basis of FTIR difference spectroscopy and site-directed mutagenesis (Braiman *et al.*, 1988a). Key features of this model are described in the text. (See Fig. 8 for revised model.)

(Fig. 5) and may be involved in linking chromophore isomerization to protein structural changes. However, in contrast to earlier studies which combined FTIR and site-directed mutagenesis, specific bands in the difference spectrum were not assignable to individual proline residues. This may indicate that either the bands assigned to proline in the difference spectrum arise from one of the eight prolines located in the loop regions of the protein or that the structural changes involving the membrane-embedded prolines are cooperatively coupled (Rothschild *et al.*, 1990b).

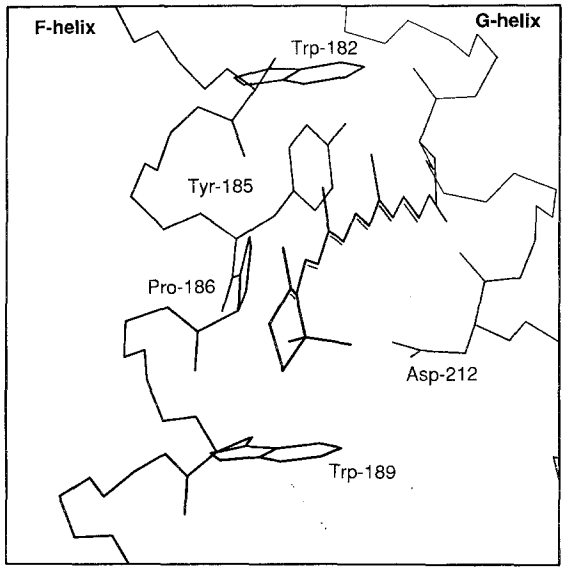

Fig. 5. The three-dimensional structural model for the interactions of the retinylidene chromophore with the putative F- and G-helices of bacteriorhodopsin from Rothschild *et al.* (1989b). Residues Trp-182, Trp-189, Tyr-185, and Pro-186 form part of a "box" which acts to constrain the possible conformations of retinal which can bind in bR. Trp-86 on helix C (not shown) was also found to participate in the binding site (Rothschild *et al.*, 1989a).

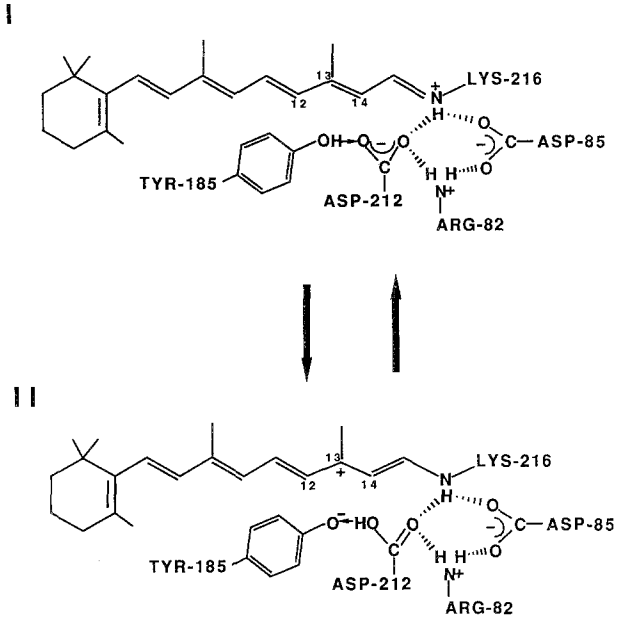

Fig. 6. Schematic model of tyrosine-185/aspartic acid 212 interactions showing two prototropic tautomers of a proposed Tyr-185/Asp-212/retinal complex. Note that the diagram is not drawn to scale or on the basis of exact coordinates (Rothschild *et al.*, 1990a).

Asp-212 Partially Protonates during M Formation

Although Asp-212 is located close to the Schiff base (see next section), its role in the bR proton pump mechanism remains undetermined. In a follow-up of an earlier study (Braiman *et al.*, 1988a), FTIR difference spectroscopy was used to investigate structural changes occurring in Asp-212 during the photocycle (Rothschild *et al.*, 1990a). Difference spectra were recorded at low temperature for the bR → K and bR → M photoreactions of the mutants D212E, D212N, and D212A. A positive 1738 cm^{-1} band which appears in the bR → M difference spectrum of wild-type bR is absent in the corresponding difference spectra of all three D212 mutants. D212A exhibited the most normal difference spectrum including the appearance of positive band at 1760 cm^{-1} assigned previously to the protonation of Asp-85. These results support the earlier assignment of the positive 1738 cm^{-1} band in the wild-type spectrum to the COOH stretch mode of Asp-212 (Braiman *et al.*, 1988a) and indicate that a partial protonation of this residue occurs during M formation.

The relatively normal frequency of the chromophore vibrations of the photocycling ground state of D212A also indicates that it does not play a major role in regulation of the color in the light-adapted species (see discussion in section on "Related Studies"). In particular, the major chromophore bands in D212A appear at an almost identical frequency to those in wild-type bR. Deviations in the frequency of chromophore bands in D212E and D212N were attributed to an increase in the amount of a 13-*cis* chromophore in the photocycling form (Rothschild *et al.*, 1989a).

In contrast to wild-type bR, which can form an M intermediate at 250 K, the mutant D212N was blocked at the L state of the photocycle (Rothschild *et al.*, 1990a), in agreement with time-resolved visible absorption measurements (Stern *et al.*, 1989; Needleman *et al.*, 1991). This may indicate that replacement of Asp-212 by Asn disrupts the active site shown in Fig. 6, preventing normal protonation of Asp-85 by the Schiff base. It was also found that mutants of Asp-212 reduced or abolished bands assigned to alterations in Tyr-185, providing further evidence for a Tyr-185/Asp-212 interaction as seen in the bR structural model deduced from electron diffraction (Henderson *et al.*, 1990).

Asp-85 Protonates during M Formation and Deprotonates during O Decay

The role of Asp-85 as the Schiff base proton

acceptor was originally postulated on the basis of low-temperature FTIR measurements made on site-directed mutants of the four membrane-embedded Asp groups (Braiman *et al.*, 1988a). In particular, the band at 1760 cm^{-1} in the bR → M difference spectrum was assigned the C=O stretch mode of the COOH of Asp-85. This model was also consistent with structure–function studies involving Asp-85 (Mogi *et al.*, 1988) (see next section) and more recently with the proximity of Asp-85 to the Schiff base in the electron-diffraction-based bR structure (Henderson *et al.*, 1990).

Recently, the application of stroboscopic time-resolved FTIR with a time resolution 50 μs (Braiman *et al.*, 1991) has allowed detection of structural changes in the early photocycle. The 1760 cm^{-1} band has a risetime which matches the deprotonation of the Schiff base consistent with its postulated role as an acceptor of the proton from the Schiff base. The data also agree with earlier single-wavelength kinetic IR measurements (Mäntele *et al.*, 1982). Although Asp-212 also protonates during this time period, the mutant D212A is able to form a relatively normal M intermediate (Rothschild *et al.*, 1990a), making it an unlikely candidate as the Schiff base proton acceptor. In addition, time-resolved FTIR reveals that Asp-212 protonates in the mutant D96A and D96E *after* M formation (Bousché *et al.*, 1992).

Recent time-resolved FTIR difference measurements also reveal that Asp-85 remains protonated during the M → N and N → O transitions, but undergoes a change in its environment as indicated by a shift of the carboxyl stretch frequency from 1761 to 1755 cm^{-1} (Braiman *et al.*, 1991; Bousché *et al.*, 1992). Thus, the proton transferred from the Schiff base to Asp-85 cannot be the same as the one released in the early photocycle to the outside medium. As seen in Fig. 4, this could be explained if proton ejection to the cytoplasmic medium is triggered by Asp-85 protonation due to disruption of an ionic interaction between Arg-82 and Asp-85 (Fig. 4).

Asp-96 Deprotonates during N Formation and Reprotonates during O Formation

The protonation state of Asp-96 in the late photocycle has been examined in several recent studies (Gerwert *et al.*, 1990b; Bousché *et al.*, 1991a, 1992; Muller *et al.*, 1991; Pfefferlé *et al.*, 1991). In one experiment, bands in the time-resolved difference spectra of bR were assigned by obtaining analogous time-resolved spectra from the site-directed mutants Asp-96 → Ala and Asp-96 → Glu (Bousché *et al.*, 1991a). While Asp-96 exists in a predominantly protonated state in the M intermediate (Braiman *et al.*, 1988a; Gerwert *et al.*, 1989), upon formation of the N intermediate it deprotonates as indicated both by an increase in the negative band at 1742 cm^{-1} assigned to the Asp-96 COOH group in wild-type bR and a negative band at 1720 cm^{-1} assigned to the Glu-96 COOH in the mutant Asp-96 → Glu (Fig. 7). This result and other FTIR studies (Gerwert *et al.*, 1990b; Braiman *et al.*, 1991; Pfefferlé *et al.*, 1991) confirm the role of Asp-96 as a key residue in the reprotonation pathway leading from the cytoplasm to the Schiff base as deduced earlier on the basis of other techniques (Butt *et al.*, 1989; Tittor *et al.*, 1989; Holz *et al.*, 1989; Otto *et al.*, 1989).

The protonation state of Asp residues in the O intermediates has also been investigated recently using a similar approach (Bousché *et al.*, 1992). Since it is difficult to stabilize this intermediate in the photocycle of wild-type bR, the mutant Tyr-185 → Phe was utilized, which at high pH exhibits a relatively normal photocycle except for the accumulation of the O intermediate in the late photocycle (Duñach *et al.*, 1990a, Sonar *et al.*, 1992). Because of this property, bands in the time-resolved FTIR difference spectra were assigned to the O chromophore and protein vibrational modes. The results show that along with the 13-*cis* → *all-trans* reisomerization of the chromophore, Asp-96 reprotonates (Table I) and the protein undergoes a partial reversal of the changes in the secondary structure that occurred earlier in the photocycle. In contrast, the active-site configuration of bR involving ionic interactions between Asp-212, Asp-85, and the Schiff base (Braiman *et al.*, 1988a) is not reestablished until the completion of the photocycle.

The Role of Thr-46 and Thr-89 in the Photocycle

The role of the residues, Thr-46 and Thr-89, in the bR photocycle was investigated by FTIR difference spectroscopy and time-resolved visible absorption spectroscopy of site-directed mutants (Rothschild *et al.*, 1992). The mutants T89D and T46V were previously studied by time-resolved visible absorption spectroscopy in DMPC/CHAPS/SDS mixed micelles (Marti *et al.*, 1991a). The FTIR

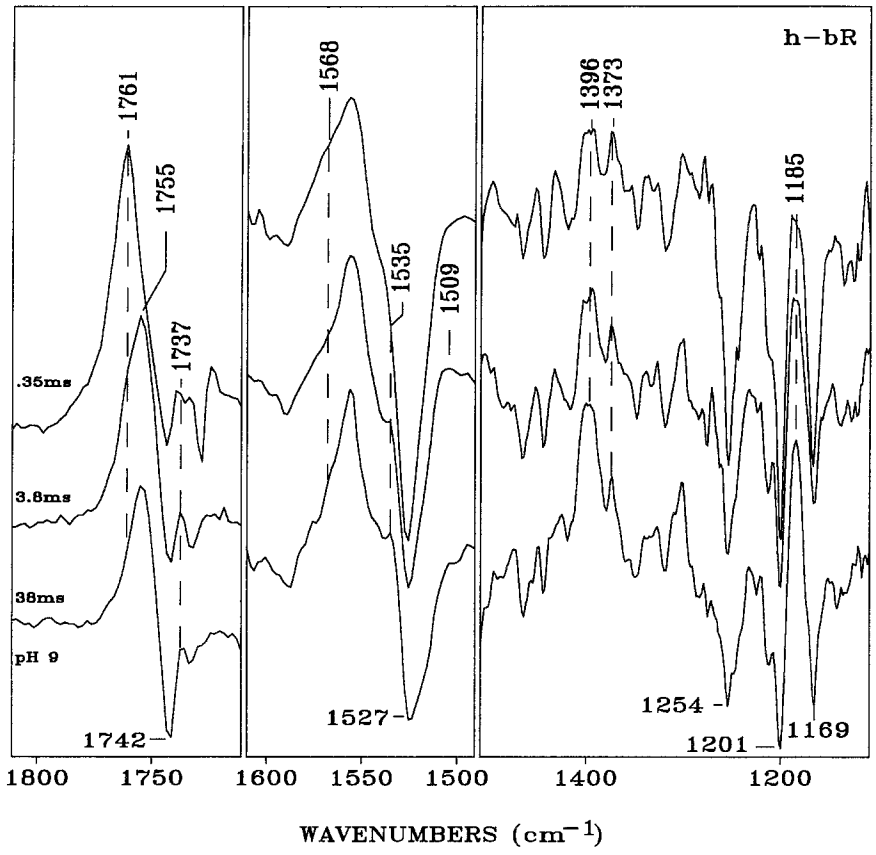

Fig. 7. Time-resolved FTIR difference spectra of purple membrane. Spectra were recorded at 297 K at 4 cm^{-1} resolution. Each spectrum represents average over 0.7 ms. The time is midpoint of time range during which spectrum was recorded. Top and middle: Sample at pH 7. Bottom: Sample at pH 9. (From Bousché *et al.*, 1991a.)

measurements revealed that the mutant T46V perturbed the state of Asp-96 in the L and M intermediates. In the case of the mutant T89D, substitution of a low-pK_a Asp residue for the high-pK_a Thr residue appeared to cause a proton transfer between Asp-89 to Asp-212 early in the photocycle. As discussed below, both these results could be explained by the existence of a transient proton-transporting network of hydrogen-bonded residues and water molecules which includes Asp-96, Thr-46, Thr-89, Tyr-185, and Asp-212.

Secondary Structural Changes during the bR Photocycle

Several bands in the 1500–1700 cm^{-1} region of the FTIR difference spectra have been assigned to the amide I and II modes (Rothschild and Clark, 1979; Rothschild and Marrero, 1982; Rothschild *et al.*, 1985; Braiman *et al.*, 1987; Roepe *et al.*, 1987a; Engelhard *et al.*, 1985; Gerwert *et al.*, 1990b; Braiman *et al.*, 1991; Bousché *et al.*, 1991a; Pfefferlé *et al.*, 1991; Ormos, 1991). In general, these bands could arise because of changes in local secondary structure involving one or more peptide bonds or changes in the orientation of secondary structure such as tilting of α-helices. For example, bands in the amide I region in the low-temperature bR → M difference spectrum have an out-of-plane dichroism, consistent with a small tilt of the net α-helix orientation away from the membrane normal (Earnest *et al.*, 1986). However, it is not possible from the data to determine if these bands involve changes in structure of one or more helices, or a more localized region of a single helix.

Information about secondary structural changes during the bR photocycle has recently been obtained

from time-resolved FTIR difference spectroscopy. In one study, it was found that structural changes occurring during the bR → M transition are partially blocked at either low temperature or low humidity (Braiman *et al.*, 1987). More recently submillisecond measurements (Braiman *et al.*, 1991) have revealed a more detailed picture, with distinctly different changes found during the L → M and M → N transition. Interestingly, bands observed in the amide I and II regions as well as the carboxyl stretch region of the bR → M and bR → N difference spectra at room temperature (Braiman *et al.*, 1991; Bousché *et al.*, 1991a) are very similar to the low-temperature difference spectra recorded at 260 and 240 K, respectively (Ormos, 1991). This similarity indicates that the two different decay modes of bR observed in the low-temperature experiments (Ormos, 1991) may reflect differences in the structure of the M and N intermediates rather than two different forms of the M intermediate (Váró and Lanyi, 1990).

DEVELOPMENT OF A MOLECULAR MODEL OF PROTON TRANSPORT

A Structure Based on Site-Directed Mutagenesis and Spectroscopy

On the basis of FTIR studies on site-directed mutants, along with structural information provided by a variety of other techniques, an increasingly detailed model for the bR pump mechanism is being developed (Braiman *et al.*, 1988a; Rothschild *et al.*, 1989a, b, 1990a, b, 1992). The structure and proton-pumping mechanism proposed in 1988 (Braiman *et al.*, 1988a) were based in part on the finding that Asp-212 and Asp-85 were both ionized and the requirement for overall charge neutrality in the interior of the protein. This led to the proposal that Asp-85, Asp-212, Arg-82, and the protonated Schiff base interact electrostatically in an active-site configuration shown in Fig. 4. Positioning Asp-85 so that it interacts with the Schiff base also places Asp-96 close to the cytoplasmic surface of the membrane. Tyr-185 from helix F was also included in this model on the basis of evidence that it interacts with the Schiff base (Braiman *et al.*, 1988b).

Additional information from FTIR spectroscopy (Braiman *et al.*, 1988a, b; Rothschild *et al.*, 1990a, b), site-directed mutagenesis (Khorana, 1988), UV/visible absorption spectroscopy (Rothschild *et al.*, 1986; Roepe *et al.*, 1987a), neutron diffraction (Seiff *et al.*, 1986; Heyn *et al.*, 1988; Hauss *et al.*, 1990), and sequence homology in helix F for bR, hR, and several rhodopsins led to the proposal that Tyr-185, Pro-186, Trp-182, and Trp-189 formed part of the retinal-binding pocket shown in Fig. 5 (Rothschild *et al.*, 1989b). The arrangement of these residues is very similar to the original coordinate map from which Fig. 4 is derived (Braiman *et al.*, 1988a). However, in contrast to the original model, the methyl groups on C_9 and C_{13} methyl groups of retinal were pointed toward the cytoplasmic side of the membrane and the NH bond toward the extracellular medium, in agreement with more recent evidence (Lin and Mathies, 1989; Hauss *et al.*, 1990). Two additional features included later were the placement of Trp-86 in the retinal-binding pocket (Rothschild *et al.*, 1989b) and a direct interaction between Asp-212 and Tyr-185 (Rothschild *et al.*, 1990a).

The success in obtaining an improved high-resolution electron-diffraction structure of bR in 1990 (Henderson *et al.*, 1990) provided strong support for almost all of the features in the spectroscopically derived model including the positioning of the aromatic residues Trp-86, Trp-182, Trp-189, Tyr-185, and the Asp residues 85, 96, and 212 (Braiman *et al.*, 1988a; Rothschild *et al.*, 1989a, b). Although the position of the Arg-82 side chain was not determined from the electron density map (Henderson *et al.*, 1990), its position in helix C allows it to interact with Asp-212 and Asp-85. The orientation of the retinylidene chromophore with its plane perpendicular to the membrane plane and polyene axis tipped approximately 20° to the vertical is also consistent with the results of polarized FTIR difference spectroscopy (Earnest *et al.*, 1986; Nabedryk and Breton, 1986) as well as visible dichroism (Heyn *et al.*, 1977; Clark *et al.*, 1980) and neutron diffraction (Seiff *et al.*, 1986; Heyn *et al.*, 1988; Hauss *et al.*, 1990).

Proton Transport

The original proton transport model illustrated in Fig. 4 was proposed in order to account for Asp protonation changes in the early photocycle deduced by FTIR (Table I). The model contained several key features (Braiman *et al.*, 1988a):

1. Asp-85 accepts a proton from the Schiff base during M formation.
2. Protonation of Asp-85 results in the ejection of a proton into the external medium as a result

of disruption of the salt bridge between Asp-85 and Arg-82.

3. Asp-96 serves both as a source of the proton that reprotonates the Schiff base, although indirectly through intermediary groups, and as a proton acceptor during proton uptake from the cytoplasmic medium.
4. Asp-212 receives a proton, possibly from Tyr-185 upon M formation. Asp-212 reprotonates the Schiff base directly during the M → N transition, receiving a proton indirectly from Asp-96.

Recently, a more comprehensive model has been proposed (Rothschild *et al.*, 1992) which retains almost all of the features of the original model but includes a more complete description of the Schiff base reprotonation pathway and protonation changes occurring during the late photocycle in Asp-85, Asp-96, and Asp-212 (Table I). In contrast to the earlier model, it uses the electron-diffraction-derived coordinates of bR (Henderson *et al.*, 1990) as well as an orientation of the Schiff base proton toward the extracellular medium (Lin and Mathies, 1989; Hauss *et al.*, 1990).

The key features of this model are shown in Fig. 8 and described below.

bR_{570}: As in the original model, Asp-212, Asp-85, Arg-82, and the protonated Schiff base interact to form an overall electrostatically neutral active site (Braiman *et al.*, 1988a). In addition, Tyr-85 interacts with Asp-212. A new feature is a network of hydrogen-bonded residues which includes water, Asp-212, Tyr-185, and Thr-89 as indicated by a series of shaded arrows in Fig. 8. This network allows a partial protonation of Asp-212 through delocalization of some of the negative charge on Asp-212 into the network, thus accounting for the partial deprotonation observed in Tyr-185 (He *et al.*, 1992a).

K_{630}: Movement of the Schiff base due to light-induced *all-trans* to 13-*cis* isomerization of the retinal chromophore disrupts the hydrogen-bonding network including the Tyr-185/Asp-212 hydrogen bond, accounting for the observed increase in the protonation state of Tyr-185 (Braiman *et al.*, 1988b; Rothschild *et al.*, 1986; Dollinger *et al.*, 1986a).

L_{550}: Asp-96 undergoes a partial deprotonation due to a protein structural change which lowers its effective pK_a. At low temperature, where the decay of the L intermediate is blocked, Asp-96 rapidly reprotonates, hence the ionized form is not directly observed. However, at room temperature, this reprotonation does not occur until M formation (Braiman *et al.*, 1991). In contrast to the earlier model, the deprotonation/reprotonation involves an unidentified internal group and not reprotonation from the internal medium which is inconsistent with measurements on the kinetics of proton uptake and release (Holz *et al.*, 1989).

M_{412}: Upon M formation, a transient network of polarizable hydrogen bonds, similar to that proposed by Zundel and coworkers (Zundel, 1986), is established which may include several water molecules along with Asp-96, Thr-46, Thr-89, Tyr-185, and Asp-212. This network in effect acts as a proton wire, increasing the protonation state of Asp-212. While none of the high-pK_a residues in this network including Tyr-185 are expected to exist in a predominantly ionized form, the polarizable hydrogen bonds allow some of the negative charge of Asp-212 to be delocalized throughout the network. In wild-type bR, the movement of positive charge toward Asp-212 is closely coupled to the transfer of the Schiff base proton to Asp-85. As a consequence of the neutralization of Asp-85, the active site is disrupted, causing an unshielding of Arg-82 and ejection of a proton to the extracellular medium as indicated in Fig. 8.

N_{550}: The M → N transition involves reprotonation of the Schiff base by a net proton transfer from Asp-96 (Holz *et al.*, 1989; Otto *et al.*, 1989; Butt *et al.*, 1989). As shown in Fig. 8, this occurs through a transient network of hydrogen-bonded residues including Asp-212, which acts as the proximal proton donor to the Schiff base. The overall process involves the transfer of a proton from Asp-212 to the Schiff base, reprotonation of Asp-212, and simultaneous donation of a proton from Asp-96 into the hydrogen-bonded network. In effect, this amounts to a net movement of a proton from Asp-96 to the Schiff base. Asp-96 is now deprotonated and no longer interacts with Thr-46, accepting a proton from the cytoplasmic medium during the next photocycle step. A partial negative charge still remains delocalized among the high-pK_a residues in the chain, while Asp-212 remains partially protonated. A second feature of the M → N transition not shown in Fig. 8 is a change in the secondary structure of bR (Braiman *et al.*, 1991). This may be directly coupled to a drop in the pK_a of Asp-96, thus accounting for its deprotonation.

O_{640}: The N → O transition involves the reprotonation of Asp-96 (Muller *et al.*, 1991; Bousché *et al.*, 1992), thus accounting for the observed slow N decay

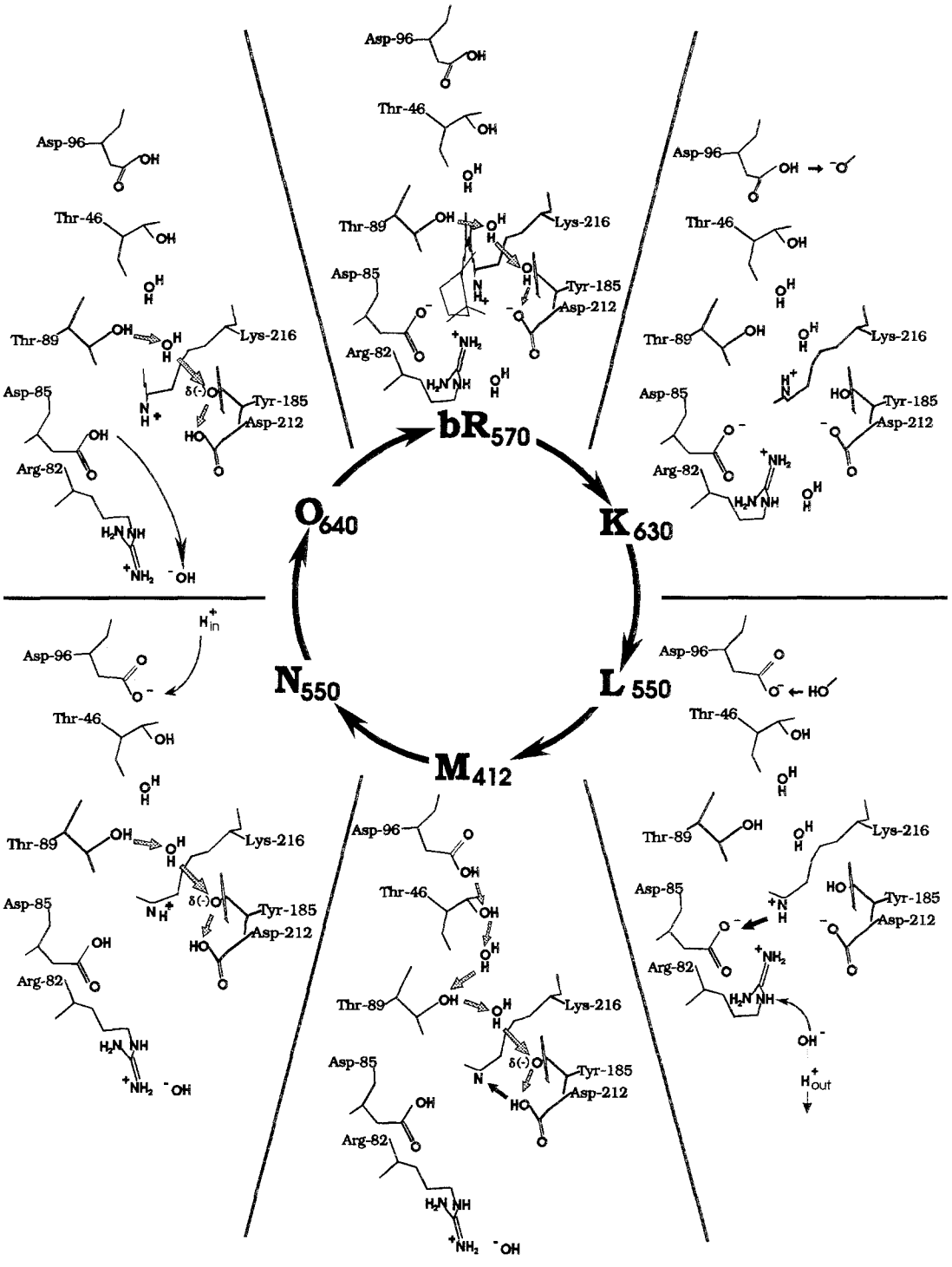

Fig. 8. Model of hydrogen-bonded proton transport network and protonation changes that occur during the bR photocycle from Rothschild *et al.* (1992). The approximate position of the residues shown is based on the coordinate map of the electron diffraction-derived bR structure (Henderson *et al.*, 1990). Single-bond rotations were allowed in the side chains of residues Asp-96, Thr-46, and Arg-82 for positional adjustments. The positions of the Schiff base nitrogen and Lys-216 side chains are approximate except in the case of the bR_{570} state. Shaded arrows denote polarizable hydrogen bonds which allow delocalization and collective movement of protons in a hydrogen-bonded network of such bonds (Zundel, 1988). In cases where a negative charge is shared among several high pK_a residues and water molecules, such as in the M intermediate, a $\delta(-)$ is shown at only one of the residues which shares the charge (i.e., Tyr-185). A black arrow is used to indicate when a net proton transfer will occur at the next step of the photocycle.

at high pH (Otto *et al.*, 1989; Kouyama *et al.*, 1988). This transition also involves a reisomerization of the chromophore from 13-*cis* to *all-trans* and a reversal of most of the secondary structural changes which occur earlier in the photocycle.

O Decay: During the O → bR transition, the ionic interactions between Asp-85, Asp-212, Arg-82, and the Schiff base are reestablished. In addition, the partial protonation of Asp-212 is reversed with the positive charge moving back toward the high-pK_a residues including Tyr-185 and Thr-89, thereby resetting the ionization states of these residues in the hydrogen-bonding network.

Related Studies

In addition to the FTIR data, the model also accounts for a variety of other data, much of which is from structure–function studies on bR. Some of these studies are discussed below:

Asp-85: Several studies have concluded that Asp-85 serves as a primary counterion to the Schiff base. As expected on the basis of a point charge model (Honig *et al.*, 1979), replacement of a negative charge by a neutral one in both D85A and D85N results in a red-shifted λ_{max} near 600 nm (Mogi *et al.*, 1988; Subramaniam *et al.*, 1990; Otto *et al.*, 1990; Needleman *et al.*, 1991, Thorgeirsson *et al.*, 1991; Marti *et al.*, 1991b). High salt concentration returns D85A to a purple form due to the substitution of an anion for Asp-85 in the active site (Marti *et al.*, 1991b). The acid-induced purple-to-blue transition can also be understood if Asp-85 becomes protonated at low pH (Subramaniam *et al.*, 1990). In fact, a positive band near 1760 cm^{-1} assigned to protonation of Asp-85 has been observed in the FTIR difference spectrum for this transition (Marrero and Rothschild, 1987a). A similar effect is likely to occur at low ionic strength due to a lowering of the surface pH (Szundi and Stoeckenius, 1989). Finally, both D85A and D85N exhibit Schiff base pK_a's near 7 compared to approximately pK_a 11 in wild-type bR in micelles, again an indication that Asp-85 acts as a primary counterion (Otto *et al.*, 1990; Marti *et al.*, 1991b).

In a recent resonance Raman study of D85N, it was found that the C=N stretching frequency downshifts 3 cm^{-1} from wild-type bR, indicating that Asp-85 is located closed to the retinal Schiff base (Lin *et al.*, 1991). In a second study based on resonance Raman spectroscopy, a 24 cm^{-1} shift was observed in the C= stretching mode of the mutant D85A along with an almost complete elimination of the H/D exchange isotope effect (P. Rath *et al.*, 1992), indicating that Asp-85 forms a hydrogen-bonding interaction with the Schiff base which is almost completely eliminated by replacement of an alanine.

A number of other structure–function studies also provide strong support for the functioning of Asp-85 as the Schiff base proton acceptor and as a key element in proton release. As expected, replacement of Asp-85 with the nonproton-accepting residues Ala and Asn abolishes proton translocation (Mogi *et al.*, 1988; Khorana, 1988; Subramaniam *et al.*, 1990). In addition, the photocycles of D85A and D85N exhibit almost no detectable M formation (Stern *et al.*, 1989; Otto *et al.*, 1990; Thorgeirsson *et al.*, 1991). Although D85N forms a small amount of a 410 nm absorbing species with a very slow risetime and decay compared to wild-type bR, this most likely reflects a less efficient deprotonation mechanism into an aqueous channel (Stern *et al.*, 1989). In contrast to D85A and D85N, D85E exhibits both proton translocation activity which is 40% of wild type (Mogi *et al.*, 1988) and formation of an M intermediate consistent with the ability of Glu to act as a substitute proton acceptor (Stern *et al.*, 1989; Otto *et al.*, 1990; Butt *et al.*, 1989).

It is interesting to note that if the direction of the Schiff base proton is toward Asp-85 as shown in Figs. 5, 6, and 8, an *all-trans* → 13-*cis* isomerization would orient the proton in the wrong direction for it to easily be transferred to Asp-85 (and for it to accept a proton from Asp-212 as discussed below). One possible explanation is that during the K → L or L → M transition an additional rotation occurs about the 14–15 C–C bond bringing the proton and Schiff base in closer proximity to Asp-85. Indeed such a rotation has been predicted on the basis of FTIR measurements (Gerwert and Siebert, 1986) and on theoretical grounds to explain the drop in the Schiff base pK_a (Schulten and Tavan, 1978). However, resonance Raman studies on the L_{550} intermediate indicate that its chromophore has a C_{14}–C_{15} *s-trans* structure (Fodor *et al.*, 1988b). An alternate explanation would be that the protein undergoes a conformational change during the L → M transition which makes the transfer of a proton to Asp-85 possible (Mathies *et al.*, 1991).

Asp-212: The role of Asp-212 as a counterion to the Schiff base is not as clear as that of Asp-85 (Mogi *et al.*, 1988). The model shown in Figs. 6 and 8 would lead to the prediction of a red-shift upon substitution of Asp-212 with a neutral residue. However, FTIR

measurements on D212A reveal that a normal chromophore with a λ_{max} near 570 nm can be formed by this mutant (Rothschild *et al.*, 1990a). In addition, in contrast to Asp-85, only a small decrease of the pK_a of the Schiff base is not found in Asp-212 mutants (Marti *et al.*, 1991b). This may indicate that the interaction of Asp-212 with the protonated Schiff base is weaker relative to Asp-85 possibly due to the effect of the nearby Arg-82 and Tyr-185 residues (Fig. 6). On the other hand, at pH > 7, a red-shifted form of D212N expressed in native *Halobacterium halobium* has been found, leading to the interpretation that Asp-212 does function as a counterion to the Schiff base in light-adapted bR (Needleman *et al.*, 1991). A red-shifted form of D212N and D212A has also been deduced from light–dark difference spectra of these mutants (Duñach *et al.*, 1990b).

The role of Asp-212 as the proximal donor group in a proton relay from Asp-96 to the Schiff base remains unestablished. This mechanism for Schiff base reprotonation was originally suggested because of the observation that it becomes protonated upon M formation and on the basis of its proximity to the Schiff base (Braiman *et al.*, 1988a). In support of this hypothesis, as seen in Fig. 8, only a small movement of the Schiff base is required in order to switch it from a position as a proton donor to Asp-85 to one of an acceptor from Asp-212. In addition, time-resolved FTIR reveals that D96A, which has a slow M decay, also exhibits a delay in the protonation of Asp-212 which normally occurs during the L $\rightarrow$ M transition (Bousché *et al.*, 1991a).

Time-resolved visible absorption studies of Asp-212 mutants have thus far provided only limited support for this concept. D212E exhibits a decrease in the M decay rate and slowed proton uptake (Otto *et al.*, 1990), as expected if Asp-212 were involved in Schiff base reprotonation. In contrast, D212A exhibits a relatively normal M decay rate (Duñach, M., Marti, T., Khorana, H. G. and Rothschild, K. J., unpublished). This might be explained if a water molecule could substitute for Asp-212 in this mutant as the proximal donor.

Asp-212 may also serve a role in the reisomerization of the chromophore as recently suggested (Rothschild *et al.*, 1990a). In particular, partial neutralization of Asp-212 in the N intermediate could lower the energy barrier for reisomerization (Seltzer, 1987). In the model shown in Fig. 8, Asp-212 is only partially protonated; thus, two distinct forms of N may exist which differ by the protonation state of Asp-212. Reisomerization would be expected to occur from the protonated form of Asp-212. However, this form might be difficult to observe in the native bR photocycle since it could be red-shifted due to neutralization of Asp-212 and thus overlap with the O intermediate which also has a red-shifted chromophore. Interestingly, the mutants L93A and L93T form a long-lived O-like and N-like intermediate in the late photocycle which are believed to be in equilibrium (Subramaniam *et al.*, 1991a). Since these substitutions could act to block reisomerization of the chromophore due to close contact between Leu-93 with the methyl group of C-13 of retinal (Henderson *et al.*, 1990), an accumulation of the red-shifted form of the N intermediate could explain the observed results.

Arg-82: The position of the side chain of Arg-82 in the bR structure remains to be established. However, several recent studies have concluded that it directly interacts with Asp-85 and Asp-212. In particular, substitution of Arg-82 with Ala or Gln causes a rise in the pK_a for the purple-to-blue transition (Stern and Khorana, 1989; Otto *et al.*, 1990; Subramaniam *et al.*, 1990; Thorgeirsson *et al.*, 1991). If this transition is associated with Asp-85 protonation in wild-type bR (Subramaniam *et al.*, 1990), then removal of Arg-82 and its interaction with an ionized Asp-85 would be expected to raise the pK_a for this reaction.

In support of Arg-82 having a role in proton release, transient pH measurements show that this release is strongly retarded in the mutants R82Q and R82A (Otto *et al.*, 1990). Because Arg-82 is replaced by neutral residues in these mutants, proton release might occur via a direct deprotonation of Asp-85 during the late stages of the photocycle. The M intermediate in R82Q and R82A has also been observed to have an accelerated rise kinetics (Otto *et al.*, 1990; Thorgeirsson *et al.*, 1991) and it has been attributed to the Asp-85 counterion having a more negative character and increased affinity for the Schiff base proton (Thorgeirsson *et al.*, 1991).

Asp-96: Although most of the focus has been on the role of Asp-96 in the late photocycle, FTIR difference spectroscopy detects changes in this residue during the K $\rightarrow$ L $\rightarrow$ M transitions (Braiman *et al.*, 1988a; Gerwert *et al.*, 1989; Braiman *et al.*, 1991). In support of a role for Asp-96 in the early photocycle, D96N affects the kinetics of L and M formation (Thorgeirsson *et al.*, 1991). Protein structural changes detected by FTIR difference spectroscopy (Gerwert

et al., 1989; Bousché *et al.*, 1991a) and the increased reactivity of hydroxylamine with the Schiff base in the early photocycle (Subramaniam *et al.*, 1991b) may be associated with these alterations in Asp-96.

Asp-96 deprotonation during the M → N transition was deduced from the photocycle kinetics of the mutants D96N and D96A, which have a pH sensitive M decay that at pH 7 and above is significantly slower than wild-type bR (Butt *et al.*, 1989; Tittor *et al.*, 1989; Stern *et al.*, 1989; Holz *et al.*, 1989; Otto *et al.*, 1989). It was concluded that in these mutants reprotonation of the Schiff base must occur through an alternate mechanism which is rate limited by the proton concentration in the external medium. In addition, proton conductivity and transient pH experiments reveal a delayed proton uptake in the late photocycle of these mutants (Marinetti *et al.*, 1989; Holz *et al.*, 1989). Time-resolved photovoltage measurements (Otto *et al.*, 1989) also established that Asp-96 plays a major role in reprotonation of the Schiff base. Recently, Asp-96 deprotonation during the M → N transition has been directly measured by several groups using static and time-resolved FTIR difference spectroscopy (Gerwert *et al.*, 1990b; Braiman *et al.*, 1991; Bousché *et al.*, 1991a; Pfefferlé *et al.*, 1991).

Asp-96 reprotonation during the N → O transition as measured by FTIR difference spectroscopy (Bousché *et al.*, 1992) is consistent with results from absorption spectroscopy (Kouyama *et al.*, 1988) and resonance Raman spectroscopy (Ames and Mathies, 1990) and time-resolved photovoltage measurements (Otto *et al.*, 1989) which show that this transition is slowed at high pH or high salt (Szundi and Stoeckenius, 1989). Under these conditions, reprotonation of Asp-96 is expected to become the rate-limiting step for the N → O transition.

The interaction of Asp-96 with other residues is also being defined by spectroscopic studies coupled with site-directed mutagenesis. Recent studies on threonine and serine mutants shows that Thr-46 and Ser-226 increase the M decay rate while slowing proton uptake, consistent with a drop in Asp-96 pK_a (Marti *et al.*, 1991b). As discussed, FTIR results are consistent with an interaction between Thr-46 and Asp-96 (Rothschild *et al.*, 1992).

SUMMARY AND FUTURE PERSPECTIVES

Progress in elucidating the molecular mechanism of proton pumping in bacteriorhodopsin illustrates the usefulness of FTIR difference spectroscopy as a physical probe of biomolecular processes. While bacteriorhodopsin was the first system to be studied using this approach, it is now being used extensively to study other membrane-based mechanisms including visual transduction in rhodopsins (Ganter *et al.*, 1988; Rothschild and DeGrip, 1987; DeGrip *et al.*, 1988) and energy conversion by photosynthetic reaction centers (Nabedryk *et al.*, 1990). The application of attenuated total reflection techniques is also facilitating the study of non-light-driven proteins inlcuding the acetylcholine receptor (Baenziger *et al.*, 1992).

In the future, FTIR difference spectroscopy can provide increasingly detailed information about proton translocation and energy transduction in bacteriorhodopsin as well as the mechanism of other membrane-based processes. Progress depends to a large extent on further assignments of specific bands in the FTIR difference spectra to vibrational modes of individual amino acid residues and peptide groups. Along with the use of site-directed mutagenesis, more powerful methods for selective incorporation of isotope labels can facilitate these assignments. Continued development of polarized and time-resolved techniques are also likely to be of significance in future FTIR studies, offering more detailed information about structural changes occurring on the submillisecond time scale.

ACKNOWLEDGMENTS

Some of the research discussed here and conducted in the author's laboratory was supported by grants from NSF (DMB-8806007), NIH (EY05499), and ONR (N00014-88-K-0464). Among the co-workers who contributed to the work reviewed here are P. L. Ahl, J. E. Baenziger, S. Berkowitz, M. Braiman, O. Bousché, M. Duñach, T. N. Earnest, J. Gillespie, D. Gray, D. During, Y. W. He, H. Marrero, P. Rath, P. Roepe, and S. Sonar. We would also like to greatly acknowledge our ongoing collaborations with the research groups of H. G. Khorana, J. Herzfeld, J. Lugtenberg, J. Spudich, and W. J. DeGrip. We especially thank M. Heyn, T. Marti, and S. Sonar for helpful discussions and critical comments on this manuscript and Y. W. He for preparation of the figures.

REFERENCES

Alben, J. O., Altschuld, R. A., Fiamingo, F. G., and Moh, P. P. (1982). In *Electron Transport and Oxygen Utilization*, Proc. Int. Symp. Interact. Iron Proteins Oxygen Electron Transp., 1980 (Ho, C., ed.), Elsevier, New York, pp. 205–208.

Ames, J. B., and Mathies, R. A. (1990). *Biochemistry* **29**, 7181–7190.

Ames, J. B., Bolton, S. R., Netto, M. M., and Mathies, R. A. (1990). *J. Am. Chem. Soc.* **112**, 9007–9009.

Aton, B., Doukas, A. G., Narva, D., Callender, R., Dinur, U., and Honig, B. (1980). *Biophys. J.* **29**, 70–94.

Baenziger, J. E., Miller, K. W., and Rothschild, K. J. (1992). *Biophys. J.*, in press.

Bagley, K., Dollinger, G., Eisenstein, L., Singh, A. K., and Zimanyi, L. (1982). *Proc. Natl. Acad. Sci. USA* **79**, 4972–4976.

Bagley, K. A., Balogh-Nair, V., Croteau, A. A., Dollinger, G., Ebrey, T. G., Eisenstein, L., Hong, M. K., Nakanishi, K., and Vittitow, J. (1985). *Biochemistry* **24**, 6055–6071.

Barth, W. K., A., and Mäntele, W. (1991). *Biophys. J.* **59**, 339a.

Birge, R. R. (1990). *Annu. Rev. Phys. Chem.* **41**, 683–733.

Birge, R. R., Zhang, C. F., and Lawrence, A. F. (1989). In *Molecular Electronics: Biosensors and Biocomputers* (Hong, F. T., ed.), Plenum Press, New York and London, pp. 369–379.

Blanck, A., and Oesterhelt, D. (1987). *EMBO J.* **6**, 265–273.

Blanck, A., Oesterhelt, D., Ferrando, E., Schegk, E. S., and Lottspeich, F. (1989). *EMBO J.* **8**, 3963–3971.

Bogomolni, R. A. (1980). In *Bioelectrochemistry* (Keyzer, H., and Gutmann, F., eds), pp. 83–95. Plenum Press, New York.

Bousché, O., Braiman, M. S., He, Y. W., Marti, T., Khorana, H. G., and Rothschild, K. J. (1991a). *J. Biol. Chem.* **266**, 11063–11067.

Bousché, O., Spudich, E. N., Spudich, J. L., and Rothschild, K. (1991b). *Biochemistry* **30**, 5395–5400.

Bousché, O., Sonar, S., Krebs, M., Khorana, H. G., and Rothschild, K. J. (1992). Submitted.

Braiman, M. S., and Rothschild, K. J. (1988). *Annu. Rev. Biophys. Biophys. Chem.* **17**, 541–570.

Braiman, M. S., and Wilson, K. J. (1989). In *Proceedings of the Seventh International Conference on Fourier and Computerized Infrared Spectroscopy*, Proc. SPIE Int. Soc. Opt. Eng. Vol. 1145, pp. 397–399.

Braiman, M. S., Ahl, P. L., and Rothschild, K. J. (1987). *Proc. Natl. Acad. Sci. USA* **84**, 5221–5225.

Braiman, M. S., Mogi, T., Marti, T., Stern, L. J., Khorana, H. G., and Rothschild, K. J. (1988a). *Biochemistry* **27**, 8516–8520.

Braiman, M. S., Mogi, T., Stern, L. J., Hackett, N. R., Chao, B. H., Khorana, H. G., and Rothschild, K. J. (1988b). *Proteins: Struct, Function, Genet.* **3**, 219–229.

Braiman, M. S., Bousché, O., & Rothschild, K. J. (1991). *Proc. Natl. Acad. Sci. USA* **88**, 2388–2392.

Brandl, C. J., and Deber, C. M. (1986). *Proc. Natl. Acad. Sci. USA* **83**, 917–921.

Breton, J., & Nabedryk, E. (1989). *Biochim. Biophys. Acta* **973**, 13–18.

Butt, H. J., Fendler, K., Bamberg, E., Tittor, J., and Oesterhelt, D. (1989). *EMBO J.* **8**, 1657–1663.

Clark, N. A., Rothschild, K. J., Luippold, D., and Simons, B. (1980). *Biophys. J.* **31**, 65–96.

DeGrip, W. J., Gillespie, J., Gray, D., Bovee, P. H. M., Lugtenburg, J., and Rothschild, K. J. (1988). *Photochem. Photobiol.* **48**, 497–504.

Diller, R., Iannone, M., Bogomolni, R., and Hochstrasser, R. M. (1991). *Biophys. J.* **60**, 286–289.

Dollinger, G., Eisenstein, L., Lin, S., Nakanishi, K., and Termini, J. (1986a). *Biochemistry* **25**, 6524–6533.

Dollinger, G., Eisenstein, L., Lin, S. L., Nakanishi, K., Odashima, K., and Termini, J. (1986b). *Methods Enzymol.* **127**, 649–662.

Downer, N. W., Bruchman, T. J., and Hazzard, J. H. (1986). *J. Biol. Chem.* **261**, 3640–3647.

Duñach, M., Berkowitz, S., Marti, T., He, Y. W., Subramaniam, S., Khorana, H. G., and Rothschild, K. J. (1990a). *J. Biol. Chem.* **265**, 16978–16984.

Duñach, M., Marti, T., Khorana, H. G., and Rothschild, K. J. (1990b). *Proc. Natl. Acad. Sci. USA* **87**, 9873–9877.

Dunker, A. K. (1982). *J. Theor. Biol.* **97**, 95–127.

Earnest, T. N., Roepe, P., Braiman, M. S., Gillespie, J., and Rothschild, K. J. (1986). *Biochemistry* **25**, 7793–7798.

Earnest, T. N., Roepe, P., Das Gupta, S. K., Herzfeld, J., and Rothschild, K. J. (1987). *Retinal Proteins*, pp. 133–143. Univ. Illinois Press, Urbana.

Earnest, T. N., Herzfeld, J., and Rothschild, K. J. (1990). *Biophys. J.* **58**, 1539–1546.

Eigen, M., and DeMayer, L. (1958). *Proc. R. Soc. London Ser. A (Math. Phys. Sci.)* **247**, 505–533.

Eisenstein, L., Lin, S., Dollinger, G., Odashima, K., Termini, J., Konno, K., Ding, W., and Nakanishi, K. (1987). *J. Am. Chem. Soc.* **109**, 6860–6862.

Engelhard, M., Gerwert, K., Hess, B., and Siebert, F. (1985) *Biochemistry* **24**, 400–407.

Fahmy, K., Siebert, F., Grossjean, M. F., and Tavan, P. (1989). *J. Mol. Struct.* **214**, 257–288.

Fodor, S. P. A., Ames, J. B., Gebhard, R., van den Berg, E. M. M., Stoeckenius, W., Lugtenburg, J., and Mathies, R. A. (1988a). *Biochemistry* **27**, 7097–7101.

Ganter, U. M., Gaertner, W., and Siebert, F. (1988). *Biochemistry* **27**, 7480–7488.

Gerwert, K., and Hess, B. (1988). In *Ion Pumps: Structure, Function and Regulation*, Alan R. Liss, Inc., New York.

Gerwert, K., and Siebert, F. (1986). *EMBO J.* **5**, 805–811.

Gerwert, K., Siebert, F., Pardoen, J. A., Winkel, C., and Lugtenburg, J. (1985). In *Time-Resolved Vibrational Spectroscopy (Springer Proc. Phys. 4)* (Laubereau, A., and Stockburger, M., eds), Springer Verlag, Berlin-Heidelberg-New York, pp. 259–262.

Gerwert, K., Hess, B., Soppa, J., and Oesterhelt, D. (1989). *Proc. Natl. Acad. Sci. USA* **86**, 4943–4947.

Gerwert, K., Hess, B., and Engelhard, M. (1990a). *FEBS Lett.* **261**, 449–454.

Gerwert, K., Souvignier, G., and Hess, B. (1990b). *Proc. Natl. Acad. Sci. USA* **87**, 9774–9778.

Gibson, N. J., and Cassim, J. Y. (1989). *Biochemistry* **28**, 2134–2139.

Glaeser, R. M., Downing, K. H., and Jap, B. K. (1991). *Biophys. J.* **59**, 934–938.

Griffiths, P. R., and de Haseth, J. A. (1986). *Fourier Transform Infrared Spectrometry*, (Volume 83 of *Chemical Analysis*), Wiley/Interscience, New York, pp. 386–425.

Hampp, N., Bräuchle, C., and Oesterhelt, D. (1990). *Biophys. J.* **58**, 83–93.

Hanamoto, J. H., Dupuis, P., and El-Sayed, M. A. (1984). *Proc. Natl. Acad. Sci. USA* **81**, 7083–7087.

Harada, I., Yamagishi, T., Uchida, K., and Takeuchi, H. (1990). *J. Am. Chem. Soc.* **112**, 2443–2445.

Haris, P. I., and Chapman, D. (1988). *Biochim. Biophys. Acta* **943**, 375–380.

Haronian, D., and Lewis, A. (1991). *Appl. Opt.* **30**, 597–608.

Hauss, T., Grzesiek, S., Otto, H., Westerhausen, J., and Heyn, M. P. (1990). *Biochemistry* **29**, 4904–4913.

He, Y., Krebs, M., Khorana, H., and Rothschild, K. (1992a). *SPIE*, in press.

He, Y., Krebs, M., Herzfeld, J., Khorana, H. G., and Rothschild, K. J. (1992b). *Biophys. J.* **62**, 533a.

Henderson, R., and Unwin, P. N. T. (1975). *Nature (London)* **257**, 28–32.

Henderson, R., Baldwin, J. M., Ceska, T., Zemlin, F., Beckmann, E., and Downing, K. H. (1990). *J. Mol. Biol.* **213**, 899–929.
Herzfeld, J., Das Gupta, S. K., Farrar, M. R., Harbison, G. S., McDermott, A., Pelletier, S. L., Raleigh, D. P., Smith, S. O., Winkel, C., Lugtenburg, J., and Griffin, R. G. (1990). *Biochemistry* **29**, 5567–5574.
Heyn, M. P., Cherry, R. J., and Muller, U. (1977). *J. Mol. Biol.* **117**, 607–620.
Heyn, M. P., Westerhausen, J., Wallat, I., and Seiff, F. (1988). *Proc. Natl. Acad. Sci. USA* **85**, 2146–2150.
Holz, M., Drachev, L. A., Mogi, T., Otto, H., Kaulen, A. D., Heyn, M. P., Skulachev, V. P., and Khorana, H. G. (1989). *Proc. Natl. Acad. Sci. USA* **86**, 2167–2171.
Honig, B., Dinur, V., Nakanishi, K., Blogh-Nair, V., Gawinowicz, M. A., Arnaboldi, M., and Motto, M. G. (1979). *J. Am. Chem. Soc.* **101**, 2503–2507.
Hunt, J. F., Earnest, T. N., Engleman, D. M., and Rothschild, K. J. (1988). *Biophys. J.* **53**, 97a.
Hunt, J. F., Bousché, O., Meyners, K. M., Rothschild, K. J., and Engelman, D. M. (1991). *Biophys. J.* **59**, 400a.
Jap, B. K., Maestre, M. F., Hayward, S. B., and Glaeser, R. M. (1983). *Biophys. J.* **43**, 81–89.
Kalisky, O., Feitelson, J., and Ottolenghi, M. (1981). *Biochemistry* **20**, 205–209.
Khorana, H. G. (1988). *J. Biol. Chem.* **263**, 7439–7442.
Kitagawa, T., and Maeda, A. (1989). *Photochem. Photobiol.* **50**, 883–894.
Kouyama, T., Nasuda-Kouyama, A., Ikegami, A., Mathew, M. K., and Stoeckenius, W. (1988). *Biochemistry* **27**, 5855–5863.
Krimm, S., and Dwivedi, A. M. (1982). *Science* **216**, 407–408.
Lee, D. C., Hayward, J. A., Restall, C. J., and Chapman, D. (1985). *Biochemistry* **24**, 4364–4373.
Lin, S. W., and Mathies, R. A. (1989). *Biophys. J.* **56**, 653–660.
Lin, S., Fodor, S. P. A., Miercke, L., Shand, R., Betlach, M., Stroud, R., and Mathies, R. (1991). *Photochem. Photobiol.* **53**, 341–346.
Lohrmann, R., Grieger, I., and Stockburger, M. (1991). *J. Phys. Chem.* **95**, 1993–2001.
Mäntele, W., Siebert, F., and Kreutz, W. (1982). In *Methods Enzymol.* **88**, 729–740.
Marinetti, T., Subramaniam, S., Mogi, T., Marti, T., and Khorana, H. G. (1989). *Proc. Natl. Acad. Sci. USA* **86**, 529–533.
Marrero, H., and Rothschild, K. J. (1987a). *FEBS Lett.* **223**, 289–293.
Marrero, H., and Rothschild, K. J. (1987b). *Biophys. J.* **52**, 629–635.
Marti, T., Otto, H., Mogi, T., Rösselet, S. J., Heyn, M. P., and Khorana, H. G. (1991a). *J. Biol. Chem.* **266**, 6919–6927.
Marti, T., Rösselet, S. J., Otto, H., Heyn, M. P., and Khorana, H. G. (1991b). *J. Biol. Chem.* **266**, 18674–18683.
Mathies, R. A., Lin, S. W., Ames, J. B., and Pollard, W. T. (1991).
McMaster, E., and Lewis, A. (1988). *Biochem. Biophys. Res. Commun.* **156**, 86–91.
Mogi, T., Stern, L. J., Marti, T., Chao, B. H., and Khorana, H. G. (1988). *Proc. Natl. Acad. Sci. USA* **85**, 4148–4152.
Mogi, T., Stern, L. J., Chao, B. H., and Khorana, H. G. (1989). *J. Biol. Chem.* **264**, 14192–14196.
Muller, K. H., Butt, H. J., Bamberg, E., Fendler, K., Hess, B., Siebert, F., and Engelhard, M. (1991). *Eur. Biophys. J.* **19**, 241–251.
Nabedryk, E., and Breton, J. (1986). *FEBS Lett.* **202**, 356–360.
Nabedryk, E., Bagley, K. A., Thibodeau, D. L., Bauscher, M., Mantele, W., and Breton, J. (1990). *FEBS Lett.* **266**, 59–62.
Nagle, J. F., and Tristram-Nagle, S. (1983). *J. Membr. Biol.* **74**, 1–14.
Needleman, R., Chang, M., Ni, B., Varo, G., Fornes, J., White, S., and Lanyi, J. (1991). *J. Biol. Chem.* **266**, 11478–11484.
Ormos, P. (1991). *Proc. Natl. Acad. Sci. USA* **88**, 473–477.
Otto, H., Marti, T., Holz, M., Mogi, T., Lindau, M., Khorana, H. G., and Heyn, M. P. (1989). *Proc. Natl. Acad. Sci. USA* **86**, 9228–9232.
Otto, H., Marti, T., Holz, M., Mogi, T., Stern, L. J., Engel, F., Khorana, H. G., and Heyn, M. P. (1990). *Proc. Natl. Acad. Sci. USA* **87**, 1018–1022.
Parker, F. S. (1983). *Applications of Infrared, Raman, and Resonance Raman Spectroscopy in Biochemistry*, Plenum Press, New York.
Pfefferlé, J. M., Maeda, A., Sasaki, J., and Yoshizawa, T. (1991). *Biochemistry* **30**, 6548–6556.
Sonar, S. M., Bousche, O., He, Y. W., Rath, P., Krebs, M., Khorana, H. G., and Rothschild, K. J. (1992). *Biophys. J.* **62**, 531a.
Rath, P., Marti, T., Khorana, H. G., and Rothschild, K. J. (1992). *Biophys. J.* **62**, 533a.
Rayfield, G. W. (1989) In *Molecular Electronics: Biosensors and Biocomputers* (Hong, F. T., ed.), Plenum Press, New York and London, pp. 361–368.
Rodman, H. S., Honig, B. H., Croteau, A., Zarrilli, G., and Nakanishi, K. (1990). *Biophys. J.* **53**, 261–269.
Roepe, P., Ahl, P. L., Das Gupta, S. K., Herzfeld, J., and Rothschild, K. J. (1987a). *Biochemistry* **26**, 6696–6707.
Roepe, P., Scherrer, P., Ahl, P. L., Das Gupta, S. K., Bogomolni, R. A., Herzfeld, J., and Rothschild, K. J. (1987b). *Biochemistry* **26**, 6708–6717.
Roepe, P., Gray, D., Lugtenburg, J., van den Berg, E. M. M., Herzfeld, J., and Rothschild, K. J. (1988a). *J. Am. Chem. Soc.* **110**, 7223–7224.
Roepe, P. D., Ahl, P. L., Herzfeld, J., Lugtenburg, J., and Rothschild, K. J. (1988b). *J. Biol. Chem.* **263**, 5110–5117.
Rothschild, K. J. (1988). *Photochemistry Photobiol.* **47**, 883–887.
Rothschild, K. J., and Clark, N. A. (1979). *Biophys. J.* **25**, 473–488.
Rothschild, K. J., and DeGrip, W. J. (1987). *Photobiochem. Photobiophys.* **13**, 245–258.
Rothschild, K. J., and Marrero, H. (1982). *Proc. Natl. Acad. Sci. USA* **79**, 4045–4049.
Rothschild, K. J., Sanches, R., Hsiao, T. L., and Clark, N. A. (1980). *Biophys. J.* **31**, 53–64.
Rothschild, K. J., Zagaeski, M., and Cantore, B. (1981). *Biochem. Biophys. Res. Commun.* **103**, 483–489.
Rothschild, K. J., Cantore, W. A., and Marrero, H. (1983). *Science* **219**, 1333–1335.
Rothschild, K. J., Marrero, H., Braiman, M., and Mathies, R. (1984a). *Photochem. Photobiol.* **40**, 675–679.
Rothschild, K. J., Roepe, P., Lugtenburg, J., and Pardoen, J. A. (1984b). *Biochemistry* **23**, 6103–6109.
Rothschild, K. J., Roepe, P., and Gillespie, J. (1985). *Biochim. Biophys. Acta* **808**, 140–148.
Rothschild, K. J., Roepe, P., Ahl, P. A., Earnest, T., Bogomolni, R. A., DasGupta, S. K., Mulliken, C. M., and Herzfeld, J. (1986). *Proc. Natl. Acad. Sci. USA* **83**, 347–351.
Rothschild, K. J., Bousché, O., Braiman, M. S., Hasselbacher, C. A., and Spudich, J. L. (1988). *Biochemistry* **27**, 2420–2424.
Rothschild, K. J., Braiman, M. S., Mogi, T., Stern, L. J., and Khorana, H. G. (1989a). *FEBS Lett.* **250**, 448–452.
Rothschild, K. J., Gray, D., Mogi, T., Marti, T., Braiman, M. S., Stern, L. J., and Khorana, H. G. (1989b) *Biochemistry* **29**, 7052–7059.
Rothschild, K. J., He, Y. W., Gray, D., Roepe, P. D., Pelletier, S. L., Brown, R. S., and Herzfeld, J. (1989c). *Proc. Natl. Acad. Sci. USA* **86**, 9832–9835.
Rothschild, K. J., Braiman, M. S., He, Y. W., Marti, T., and Khorana, H. G. (1990a). *J. Biol. Chem.* **265**, 16985–16991.
Rothschild, K. J., He, Y., Mogi, T., Marti, T., Stern, L. J., and Khorana, H. G. (1990b). *Biochemistry* **29**, 5954–5960.
Rothschild, K., He, Y. W., Sonar, S., Marti, T., and Khorana, H. G. (1992). *J. Biol. Chem.* **266**, **267**, 1615–1622.

Schulten, K., and Tavan, P. (1978). *Nature* **272**, 85–86.
Seiff, F., Wallat, I., Westerhausen, J., and Heyn, M. P. (1986). *Biophys. J.* **50**, 629–635.
Seltzer, S. (1987). *J. Am. Chem. Soc.* **109**, 1627–1631.
Siebert, F., and Mäntele, W. (1983). *Eur. J. Biochem.* **130**, 565–573.
Siebert, F., Mäntele, W., and Gerwert, K. (1983). *Eur. J. Biochem.* **136**, 119–127.
Smith, S. O., Lugtenburg, J., and Mathies, R. A. (1985). *J. Membr. Biol.* **85**, 95–109.
Stern, L. J., and Khorana, H. G. (1989). *J. Biol. Chem.* **264**, 14202–14208.
Stern, L. J., Ahl, P. L., Marti, T., Mogi, T., Duñach, M., Berkowitz, S., Rothschild, K. J., and Khorana, H. G. (1989). *Biochemistry* **28**, 10035–10042.
Subramaniam, S., Marti, T., and Khorana, H. G. (1990). *Proc. Natl. Acad. Sci. USA* **87**, 1013–1017.
Subramaniam, S., Greenhalgh, D. A., Rath, P., Rothschild, K., and Khorana, H. (1991a). *Proc. Natl. Acad. Sci. USA* **88**, 6873–6877.
Subramaniam, S., Marti, T., Rösselet, S. J., Rothschild, K. J., and Khorana, H. G. (1991b). *Proc. Natl. Acad. Sci. USA* **88**, 2583–2587.
Szundi, I., and Stoeckenius, W. (1989). *Biophys. J.* **56**, 369–383.
Thorgeirsson, T. E., Milder, S. J., Miercke, L. J., Betlach, M. C., Shand, R. F., Stroud, R. M., and Kliger, D. S. (1991). *Biochemistry* **30**, 9133–9142.
Tittor, J., Soell, C., Oesterhelt, D., Butt, H., and Bamberg, E. (1989). *EMBO J.* **8**, 3477–3482.
Uehara, K., Kawai, K., and Kouyama, T. (1990). *Denki Kagaku* **58**, 1132–1135.
Uhmann, W., Becker, A., Taran, C., and Siebert, F. (1991). *Appl. Spectrosc.* **45**, 390–397.
Váró, G., and Lanyi, J. K. (1990). *Biochemistry* **29**, 2241–2250.
Venyaminov, S. Y., and Kalnin, N. N. (1990). *Biopolymers* **30**, 1243–1257.
Yang, P. W., Stewart, L. C., and Mantsch, H. H. (1987). *Biochem. Biophys. Res. Commun.* **145**, 298–302.
Zundel, G. (1986). *Methods Enzymol.* **127**, 439–455.
Zundel, G. (1988). *J. Mol. Struct.* **177**, 43–68.